Implementation of Space Vector PWM for a Two-Phase Three-leg Voltage Source Inverter

Chakrapong Charumit [1] and **Vijit Kinnares**[2], Non-members

ABSTRACT

This paper proposes the implementation of a carrier-based balanced two-phase output space vector pulsewidth modulation (SVPWM) strategy for a three-leg voltage source inverter (VSI). The principle based on analogue and digital techniques is fully described. The space vector equivalent waveforms and SVPWM patterns are generated by a digital signal processor (DSP). The correctness of the proposed method is verified by calculated and experimental results.

Keywords: Space vector pulsewidth modulation, Three-leg voltage source inverter

1. INTRODUCTION

Pulsewidth modulation (PWM) has been studied for a long period in order to achieve better characteristics such as wide linear modulation range, less switching loss, less total harmonic distortion (THD) and easy implementation[1],[2],[6],[8],[12]. Generally, a PWM inverter plays an important role in industrial and residential applications since it offers several advantages such as reduced low order harmonics, small filter size and light weight. In the past, sinusoidal pulsewidth modulation (SPWM) was commonly used for an inverter and easily implemented by an analogue technique based on a comparison between a high frequency carrier wave and a sinusoidal reference wave. Presently, digital techniques for generating PWM patterns seem to be more attracted attentions due to the advent of a microprocessor technology resulting in precision, ease of implementation and flexibility. SVPWM is well established for a three-phase system with digital implementation. The carrier-based SVPWM and digital SVPWM are equivalent [12]. The implementation of SVPWM as carrier-based PWM can be made by either an analogue circuit or a digital technique. Although, for a two phase system particularly for a three-leg inverter [2-6],[11], there are a few publications to reveal the explicit principle and mathematically modulating functions. As shown in Fig.1, a three-leg VSI providing two phase outputs is increasingly attractive for two-phase drive applications due to good dc voltage utilization, reduced total harmonic distortion of currents and availability of three-leg modules[6],[11]. PWM techniques especially based on SVPWM applicable to this three-leg configuration have been proposed in many publications [3-5],[11]. Although a SVPWM strategy for the two-phase system offers many advantages over other techniques, a mathematical approach representing equivalent space vector still has not been reported. Therefore, this paper focuses on the principle and implementation based on the mathematical approach and DSP of the balanced two-phase SVPWM applied to the three-leg VSI. The validity of the proposed method tested with a balanced resistive-inductive load and an asymmetrical parameter type two-phase induction motor is demonstrated.

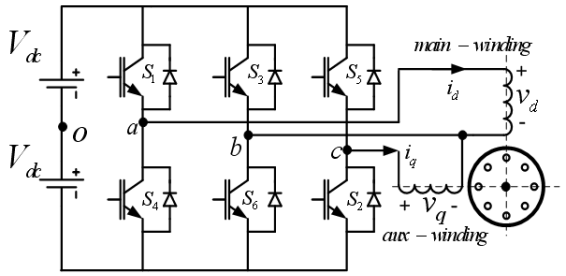

Fig.1: *Two-phase three-leg VSI supplying a two-phase induction motor*

2. TWO-PHASE SVPWM STRAEGY

The principle of a modulation strategy of carrier-based two-phase SVPWM using the three-leg VSI is illustrated in Fig.2. $v_a^{s^*}, v_b^{s^*}, v_c^{s^*}$ are space vector equivalent references of each phase leg. The mathematical equations for the space vector equivalent references will be derived and given in the next section. Switched waveforms for each leg are obtained from a comparison between a common triangular carrier wave and each space vector equivalent reference. By using phase leg b as a common phase leg, two-phase outputs are achieved from a difference of voltages between points a-b denoting as "v_d" and voltages between points c-b denoting as "v_a". The resultant fundamentals of the two phases have the same amplitude but different phase angle of 90 degrees.

Manuscript received on July 9, 2008 ; revised on November 16, 2008.

[1,2] The authors are with Department of Electrical Engineering, Faculty of Engineering, King Mongkut's Institute of Technology Ladkrabang, Bangkok, 10520, Thailand., E-mail: ch_charumit@hotmail.com and kkwijit@kmitl.ac.th

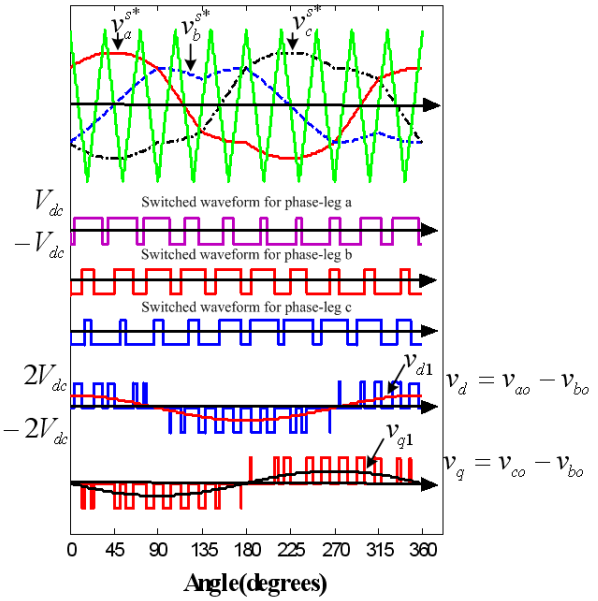

Fig.2: *Principle of the proposed carrier-based two-phase SVPWM.*

2.1 Analogue implementation

The relationship between two-phase stationary (d-q) and three-phase reference systems[3],[7] for the three-leg VSI can be written in a matrix form as

$$\begin{bmatrix} v_d^s \\ v_q^s \\ v_0 \end{bmatrix} = \begin{bmatrix} 1 & -1 & 0 \\ 0 & -1 & 1 \\ 0 & 1 & 0 \end{bmatrix} \begin{bmatrix} v_{ar} \\ v_{br} \\ v_{cr} \end{bmatrix} \tag{1}$$

where a zero sequence component (v_0) is equal to v_{br}. In order to achieve the phase difference angle between v_d^s and v_q^s is 90 degrees, the three phase reference signals can be expressed as

$$v_{ar} = m\sin(\omega t) \tag{2}$$

$$v_{br} = m\sin(\omega t - \frac{\pi}{2}) \tag{3}$$

$$v_{cr} = m\sin(\omega t - \pi) \tag{4}$$

where
m = Modulation index and $0 \leq m \leq 1$.

In order to obtain the required three-phase references for the three-leg VSI, a zero component is introduced. The inverse matrix of (1) which is the relationship for the transformation from a three-phase system[7] into a two-phase system is obtained as

$$\begin{bmatrix} v_a^{s^*} \\ v_b^{s^*} \\ v_c^{s^*} \end{bmatrix} = \begin{bmatrix} 1 & 0 & 1 \\ 0 & 0 & 1 \\ 0 & 1 & 1 \end{bmatrix} \begin{bmatrix} v_d^{s^*} \\ v_q^{s^*} \\ v_z \end{bmatrix} \tag{5}$$

where

$$v_a^{s^*} = v_d^{s^*} + v_z = v_{ar} - v_{br} + v_z = m\sqrt{2}\cos\left(\omega t - \frac{\pi}{4}\right) + v_z \tag{6}$$

$$v_b^{s^*} = v_z \tag{7}$$

$$v_c^{s^*} = v_q^{s^*} + v_z = v_{cr} - v_{br} + v_z = m\sqrt{2}\cos\left(\omega t - \frac{\pi}{4}\right) + v_z \tag{8}$$

$v_d^{s^*}$ = required direct axis reference
$v_q^{s^*}$ = required quadrature axis reference

$$v_z = \frac{v_{max} + v_{min}}{2} \tag{9}$$

where

$$v_{max} = Maximum\left\{v_d^{s^*}, v_q^{s^*}, 0\right\} \tag{10}$$

$$v_{min} = Minimum\left\{v_d^{s^*}, v_q^{s^*}, 0\right\} \tag{11}$$

The max/min expression centres the sinusoidal reference defined in (10-11) around zero at all times. In order to achieve the switching patterns of the SVPWM strategy as shown in Fig.2, a simple circuit for implementing space vector equivalent references can be designed in accordance with (1)-(11), as shown in Fig.3. The desired two-phase references are rectified to produce their envelope magnitude, this magnitude is scaled by 0.5 and is then added as an offset to each voltage reference. The voltage drop across bridge diodes is compensated by R_{Comp}. The fundamental output voltages of the main power circuit can be derived based on (6-8) as

$$v_{d1} = \overbrace{m\sqrt{2}V_{dc}}^{Amplitude}\cos\left(\omega t - \frac{\pi}{4}\right) \tag{12}$$

$$v_{q1} = \overbrace{m\sqrt{2}V_{dc}}^{Amplitude}\cos\left(\omega t + \frac{\pi}{4}\right) \tag{13}$$

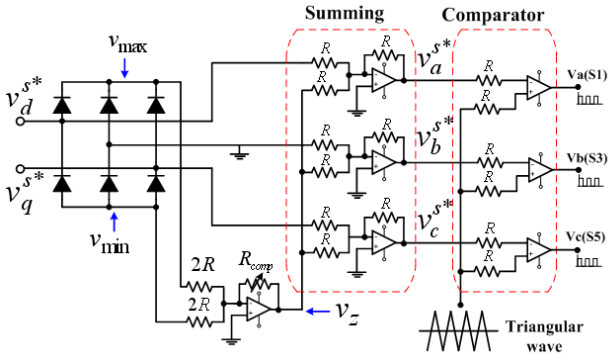

Fig.3: *Naturally sampled analogue space vector modulator.*

Waveforms obtained from (9)-(11) can be plotted as shown in Fig. 4. The resultant space vector equivalent waveforms ($v_a^{s^*}, v_b^{s^*}, v_c^{s^*}$) are illustrated in Fig.5

which will be used to compare with the common triangular carrier for generating SVPWM patterns. It is noted that these waveforms are non-sinusoidal due to the contamination of the zero signal. Space vector equivalent waveforms of phases a and b are out of phase. The difference between these phase leg references gives the two phase output references (i.e. $v_d^{s^*} = v_a^{s^*} - v_b^{s^*}$,$v_q^{s^*} = v_c^{s^*} - v_b^{s^*}$) as shown in Fig.5.

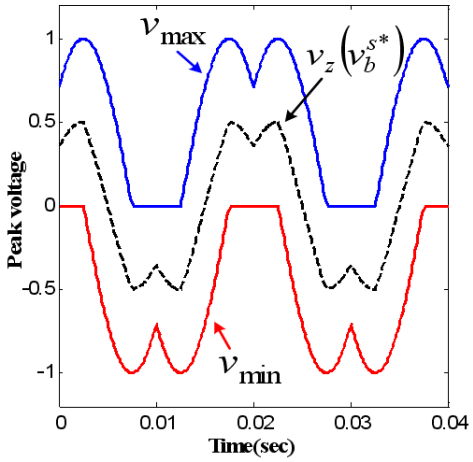

Fig.4: *Corresponding waveforms at various points of the proposed analog circuit.*

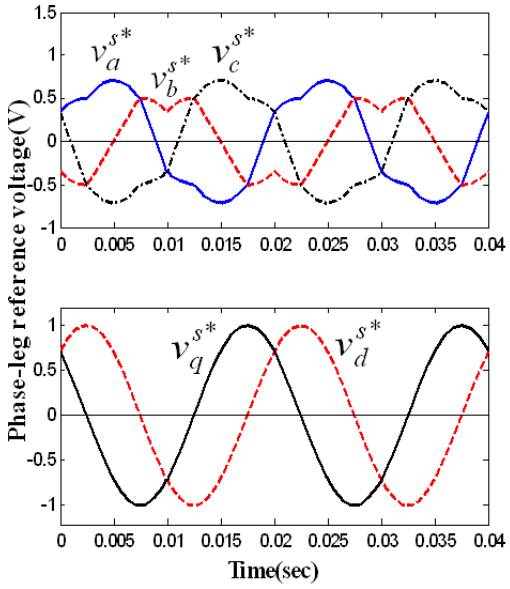

Fig.5: *Phase leg reference and two-phase reference waveforms*

2.2 Digital implementation

The principle of the two-phase SVPWM for the three-leg VSI is derived from the conventional three-phase space vector modulation which divides into six hexagonal sectors with 60 degrees displacement for each sector [3],[8]. For the two-phase SVPWM, the common leg is used. As a result, voltages between legs provide two-phase outputs, namely v_{ab} as the main winding voltage (v_d) and v_{cb} as the auxiliary winding voltage (v_q). In the switching states of SVPWM, the upper switches S_1, S_3 and S_5 of the main power circuit are assigned with either "1" or "0" equal to turn-on and turn-off, respectively. The lower switches S_4, S_6 and S_2 are opposite states against the upper switches in the same leg. The DC bus voltage is $2V_{dc}$. The switching states, corresponding output voltages and space vectors are shown in Table 1.

Table 1: *Switching patterns, output voltages and space vectors in d-q plane*

S1	S3	S5	V_d	V_q	$\overline{SV_n}$
0	0	0	0	0	$\overline{SV_0}$
1	0	0	$2V_{dc}$	0	$\overline{SV_1}$
1	1	0	0	$-2V_{dc}$	$\overline{SV_2}$
0	1	0	$-2V_{dc}$	$-2V_{dc}$	$\overline{SV_3}$
0	1	1	$-2V_{dc}$	0	$\overline{SV_4}$
0	0	1	0	$2V_{dc}$	$\overline{SV_5}$
1	0	1	$2V_{dc}$	$2V_{dc}$	$\overline{SV_6}$
1	1	1	0	0	$\overline{SV_7}$

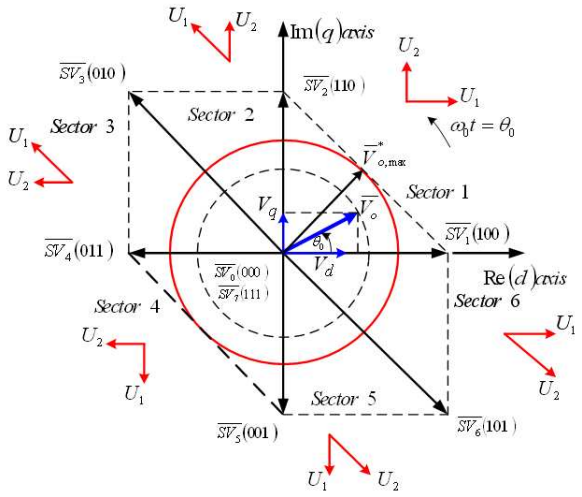

Fig.6: *Eight possible stationary voltage vectors*

As shown in Fig.6, there are six possible voltage vectors ($\overline{SV_1}, \overline{SV_2} \ldots \overline{SV_6}$). and two null vectors ($\overline{SV_0}, \overline{SV_7}$) Four active vectors ($\overline{SV_1}, \overline{SV_2}, \overline{SV_4}, \overline{SV_5}$)have a length of $2V_{dc}$ and two active vectors ($\overline{SV_3}, \overline{SV_6}$) have a length of $2\sqrt{2}V_{dc}$. Desired output voltage space vector V_o^* in a vector form, which is a rotating vector with a circular trajectory, can be calculated in terms of the average of a number of these space vectors within a half carrier period in each sector as

$$\overline{V_o^*} = v_o \angle \theta_0 = \frac{T_1}{\Delta T/2}\overline{U_1} + \frac{T_2}{\Delta T/2}\overline{U_2} \qquad (14)$$

$$\overline{U_1} = V_1 e^{j\alpha_1} \qquad (15)$$

$$\overline{U_2} = V_2 e^{j\alpha_2} \tag{16}$$

$$\frac{\Delta T}{2} = T_1 + T_2 + T_{SV0} + T_{SV7} \tag{17}$$

where $\overline{U_1}$ and $\overline{U_2}$ are the two adjacent vectors; V_1, V_2 are the magnitudes of the space vectors; θ_0 is sapling position; α_1, α_2 are angles for the two adjacent vectors; T_1, T_2 are active times for the two adjacent vectors; T_{SV0}, T_{SV7} are times for null vectors; ΔT is a carrier period. Generally, for a symmetric space vector pulse pattern, space vector times for each zero switching state (T_{SV0}, T_{SV7}) are set to be equal. The relationship between active times and the desired output voltage for each sector can be expressed in a matrix form as

$$\begin{bmatrix} \frac{T_1}{\Delta T/2} V_1 \\ \frac{T_2}{\Delta T/2} V_2 \end{bmatrix} = \frac{V_o}{\sin(\alpha_2 - \alpha_1)} \begin{bmatrix} \sin(\alpha_2 - \theta_0 \\ \sin(\theta_0 - \alpha_1 \end{bmatrix} \tag{18}$$

Active space vectors, magnitude and location for all sectors are shown in table 2.

Table 2: *Definitions for Vectors $\overline{U}_1$ and $\overline{U}_2$ of SVPWM*

Sector	$\overline{U_1}$	$\overline{U_2}$	V_1	V_2	α_1	α_2
1	$\overline{SV_1}$	$\overline{SV_2}$	$2V_{dc}$	$2V_{dc}$	0	$\pi/2$
2	$\overline{SV_3}$	$\overline{SV_2}$	$2\sqrt{2}V_{dc}$	$2V_{dc}$	$3\pi/4$	$\pi/2$
3	$\overline{SV_3}$	$\overline{SV_4}$	$2\sqrt{2}V_{dc}$	$2V_{dc}$	$3\pi/4$	π
4	$\overline{SV_5}$	$\overline{SV_4}$	$2V_{dc}$	$2V_{dc}$	$3\pi/2$	π
5	$\overline{SV_5}$	$\overline{SV_6}$	$2V_{dc}$	$2\sqrt{2}V_{dc}$	$3\pi/2$	$7\pi/4$
6	$\overline{SV_1}$	$\overline{SV_6}$	$2V_{dc}$	$2\sqrt{2}V_{dc}$	2π	$7\pi/4$

By using (18) together with Table 2, space vector active times T_{SV1}, T_{SV2} for sector 1 are arranged as follows.

$$T_{SV_1} = \frac{M}{2} \sin\left(\frac{\pi}{2} - \theta_0\right) \frac{\Delta T}{2} \tag{19}$$

$$T_{SV_2} = \frac{M}{2} \sin\left(\theta_0\right) \frac{\Delta T}{2} \tag{20}$$

where
$M = \frac{V_o}{V_{dc}}$which is the modulation index.

It is noted that $T_{SV_1} + T_{SV_2} \leq \frac{\Delta T}{2}$. Using (19) and (20) yields

$$\frac{T_{SV_1} + T_{SV_2}}{\Delta T/2} = \frac{\sqrt{2}V_o}{2V_{dc}} \cos\left(\frac{\pi}{4} - \theta_0\right) \leq 1 \tag{21}$$

From (21), the condition for maximum possible magnitude of
$overline V^*_{o,max}$ occurs at $\theta_0 = \pi/4$ which gives $V_o = \sqrt{2}V_{dc}$. As a consequence, $0 \leq M \leq \sqrt{2}$. The maximum phase voltage is approximately 70 % of DC-link voltage [4],[5]. This characteristic is one of the major advantages of the three-leg VSI.

3. MODULATING FUNCTIONS

In order to identify modulating functions of the SVPWM, the calculation of switching times for the overall sector in a period is performed.

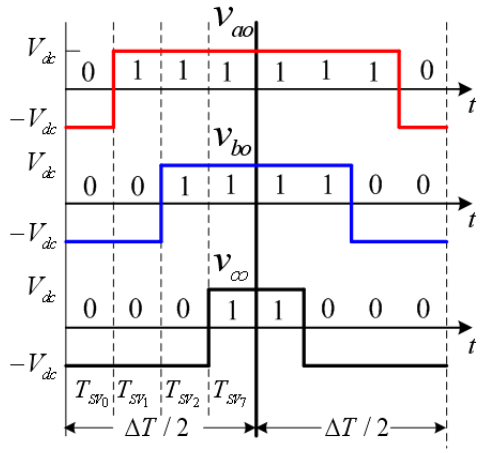

Fig.7: *Pulse pattern for the first sextant*

Fig.7 shows example of the pulse patterns of the phase leg voltages with respect to the midpoint of the DC link voltage, corresponding space vector states, and space vector times in the first sector for the conventional space vector PWM with equally spaced zero space vector $\overline{SV_0}$ and $\overline{SV_7}$. The reference (average) values for the three-phase leg voltages over the time interval $\Delta T/2$, which have a switching sequence for sector 1 in a half period of switching as $\overline{SV_0} \rightarrow \overline{SV_1} \rightarrow \overline{SV_2} \rightarrow \overline{SV_7}$ [8] are

$$v_{ao} = V_{dc}\left[\frac{T_{SV1}}{\Delta T/2} + \frac{T_{SV2}}{\Delta T/2}\right] \tag{22}$$

$$v_{bo} = V_{dc}\left[-\frac{T_{SV1}}{\Delta T/2} + \frac{T_{SV2}}{\Delta T/2}\right] \tag{23}$$

$$v_{co} = V_{dc}\left[-\frac{T_{SV1}}{\Delta T/2} - \frac{T_{SV2}}{\Delta T/2}\right] \tag{24}$$

By substituting (19-20) into (22-24), phase leg reference voltages with respect to the midpoint of the DC link voltage, which are modulating functions representing equivalent space vectors, can be expressed as

$$\frac{v_{ao}}{V_{dc}} = \frac{M}{2}\left[\sin\left(\frac{\pi}{2} - \theta_0\right) + \sin(\theta_0)\right] \tag{25}$$

$$\frac{v_{bo}}{V_{dc}} = \frac{M}{2}\left[-\sin\left(\frac{\pi}{2} - \theta_0\right) + \sin(\theta_0)\right] \tag{26}$$

$$\frac{v_{co}}{V_{dc}} = \frac{-M}{2}\left[\sin\left(\frac{\pi}{2} - \theta_0\right) + \sin(\theta_0)\right] \tag{27}$$

Similarly, according to Table 2 and (18), with the same process, space vector active times and modulating functions for the remaining sectors can be

achieved as shown in Table 3. Switching times T_1, T_2 and T_3 in the half period of the carrier for maximum $M = \sqrt{2}$ can be plotted as shown in Fig.8. Corresponding phase leg reference voltage waveforms can be shown in Fig.9. These are space vector equivalent waveforms which will be used to compare with the common triangular carrier to generate PWM patterns.

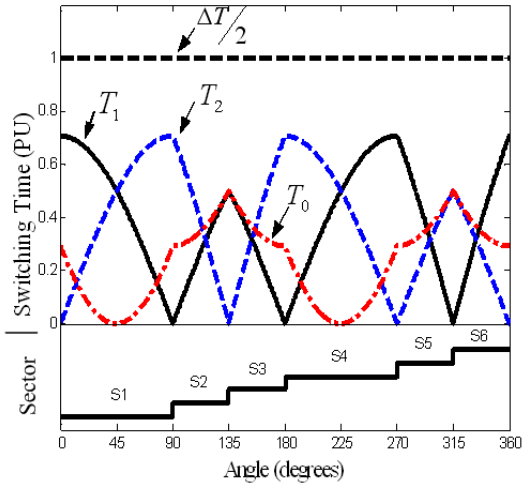

Fig.8: *Switching times and corresponding sectors*

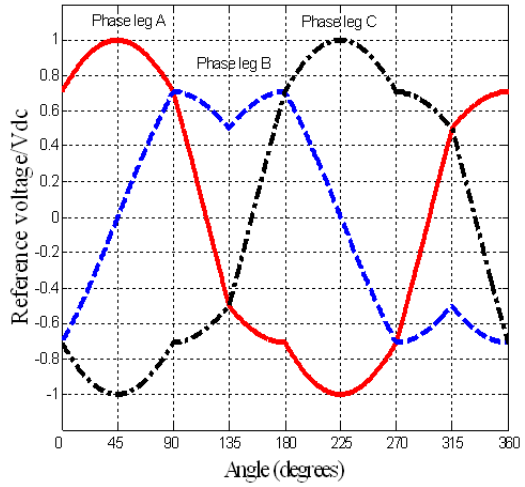

Fig.9: *Calculated reference voltages of phase leg a, b, and c for* $M = \sqrt{2}$

4. EXPERIMENTAL RESULTS

Reference voltage waveforms and SVPWM patterns are generated by using a dSPACE, DSP controller board DS1104. The board consists of a digital signal processor TMS320F240. The three leg IGBT inverter is used with switching frequency of 5kHz and dc link voltage of 300V. The R-L load (R=24 Ω, L=426mH) for a balanced load case and an asymmetrical parameter type two-phase induction motor for an unbalanced load case (see parameters in Appendix A) are used.

Table 3: *Switching times and modulating functions for overall sectors.*

	Switching times	Phase leg reference voltages
Sector 1	$\frac{T_{sy_1}}{\Delta T/2} = \frac{M}{2}\sin\left(\frac{\pi}{2} - \theta_0\right)$ $\frac{T_{sy_2}}{\Delta T/2} = \frac{M}{2}\sin(\theta_0)$	$\frac{v_{ao}}{V_{dc}} = \frac{M}{2}\left[\sin\left(\pi/2 - \theta_0\right) + \sin(\theta_0)\right]$ $\frac{v_{bo}}{V_{dc}} = \frac{M}{2}\left[-\sin\left(\pi/2 - \theta_0\right) + \sin(\theta_0)\right]$ $\frac{v_{co}}{V_{dc}} = \frac{-M}{2}\left[\sin\left(\pi/2 - \theta_0\right) + \sin(\theta_0)\right]$
Sector 2	$\frac{T_{sy_2}}{\Delta T/2} = \frac{M\sqrt{2}}{2}\sin\left(\frac{3\pi}{4} - \theta_0\right)$ $\frac{T_{sy_3}}{\Delta T/2} = \frac{M}{2}\sin\left(\theta_0 - \frac{\pi}{2}\right)$	$\frac{v_{ao}}{V_{dc}} = \frac{M}{2}\left[-\sin\left(\theta_0 - \pi/2\right) + \sqrt{2}\sin\left(3\pi/4 - \theta_0\right)\right]$ $\frac{v_{bo}}{V_{dc}} = \frac{M}{2}\left[\sin\left(\theta_0 - \pi/2\right) + \sqrt{2}\sin\left(3\pi/4 - \theta_0\right)\right]$ $\frac{v_{co}}{V_{dc}} = \frac{-M}{2}\left[\sin\left(\theta_0 - \pi/2\right) + \sqrt{2}\sin\left(3\pi/4 - \theta_0\right)\right]$
Sector 3	$\frac{T_{sy_3}}{\Delta T/2} = \frac{M}{2}\sin(\pi - \theta_0)$ $\frac{T_{sy_4}}{\Delta T/2} = \frac{M\sqrt{2}}{2}\sin\left(\theta_0 - \frac{3\pi}{4}\right)$	$\frac{v_{ao}}{V_{dc}} = \frac{-M}{2}\left[\sin(\pi - \theta_0) + \sqrt{2}\sin\left(\theta_0 - 3\pi/4\right)\right]$ $\frac{v_{bo}}{V_{dc}} = \frac{M}{2}\left[\sin(\pi - \theta_0) + \sqrt{2}\sin\left(\theta_0 - 3\pi/4\right)\right]$ $\frac{v_{co}}{V_{dc}} = \frac{M}{2}\left[-\sin(\pi - \theta_0) + \sqrt{2}\sin\left(\theta_0 - 3\pi/4\right)\right]$
Sector 4	$\frac{T_{sy_4}}{\Delta T/2} = \frac{M}{2}\sin\left(3\pi/2 - \theta_0\right)$ $\frac{T_{sy_5}}{\Delta T/2} = \frac{M}{2}\sin(\theta_0 - \pi)$	$\frac{v_{ao}}{V_{dc}} = \frac{-M}{2}\left[\sin(\theta_0 - \pi) + \sin\left(3\pi/2 - \theta_0\right)\right]$ $\frac{v_{bo}}{V_{dc}} = \frac{M}{2}\left[-\sin(\theta_0 - \pi) + \sin\left(3\pi/2 - \theta_0\right)\right]$ $\frac{v_{co}}{V_{dc}} = \frac{M}{2}\left[\sin(\theta_0 - \pi) + \sin\left(3\pi/2 - \theta_0\right)\right]$
Sector 5	$\frac{T_{sy_5}}{\Delta T/2} = \frac{M\sqrt{2}}{2}\sin\left(\frac{7\pi}{4} - \theta_0\right)$ $\frac{T_{sy_6}}{\Delta T/2} = \frac{M}{2}\sin\left(\theta_0 - \frac{3\pi}{2}\right)$	$\frac{v_{ao}}{V_{dc}} = \frac{M}{2}\left[-\sqrt{2}\sin\left(7\pi/4 - \theta_0\right) + \sin\left(\theta_0 - 3\pi/2\right)\right]$ $\frac{v_{bo}}{V_{dc}} = \frac{-M}{2}\left[\sqrt{2}\sin\left(7\pi/4 - \theta_0\right) + \sin\left(\theta_0 - 3\pi/2\right)\right]$ $\frac{v_{co}}{V_{dc}} = \frac{M}{2}\left[\sqrt{2}\sin\left(7\pi/4 - \theta_0\right) + \sin\left(\theta_0 - 3\pi/2\right)\right]$
Sector 6	$\frac{T_{sy_6}}{\Delta T/2} = \frac{M}{2}\sin(2\pi - \theta_0)$ $\frac{T_{sy_1}}{\Delta T/2} = \frac{M\sqrt{2}}{2}\sin\left(\theta_0 - \frac{7\pi}{4}\right)$	$\frac{v_{ao}}{V_{dc}} = \frac{M}{2}\left[\sqrt{2}\sin\left(\theta_0 - 7\pi/4\right) + \sin(2\pi - \theta_0)\right]$ $\frac{v_{bo}}{V_{dc}} = \frac{-M}{2}\left[\sqrt{2}\sin\left(\theta_0 - 7\pi/4\right) + \sin(2\pi - \theta_0)\right]$ $\frac{v_{co}}{V_{dc}} = \frac{M}{2}\left[-\sqrt{2}\sin\left(\theta_0 - 7\pi/4\right) + \sin(2\pi - \theta_0)\right]$

Fig.10 shows the experimental space vector equivalent reference waveforms. It is evident that the experimental references are identical with the calculated ones as shown in Fig.9. The phase difference angle between v_a and v_c is 180 degrees (out of phase) as mentioned in the analogue implementation. Fig.11 shows the experimental two-phase output references (i.e $v_{ab} = v_a - v_b$ and $v_{cb} = v_c - v_b$) having phase difference angle of 90 degrees and sinusoidal waveforms. The reason for obtaining sinusoidal waveforms of the two-phase references is that the zero component is cancelled. These confirms the validity of the proposed technique. Output voltage and current waveforms can be shown in Fig.12 for the two-phase balanced load. Fig.13 shows corresponding circular cur-

rent vector trajectory. It can be seen that the amplitudes of the currents for each phase are equal and the phase difference angle is 90 degrees thus giving a circular shape locus due to the balanced R-L load. The phase difference angle is also 90 degrees for PWM output voltages.

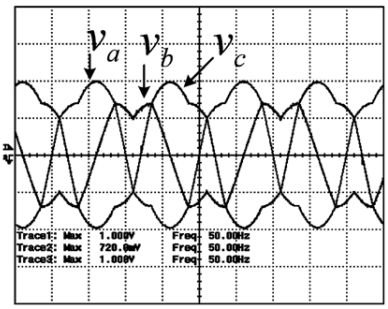

Fig.10: *Reference voltage waveforms for phase-legs (500mV/div, 5ms/div)*

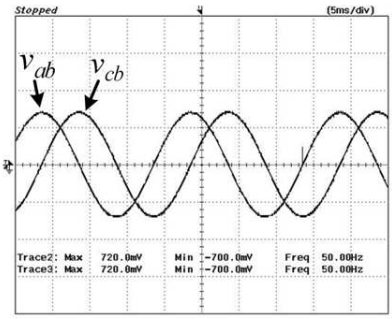

Fig.11: *Two-phase Reference waveforms*

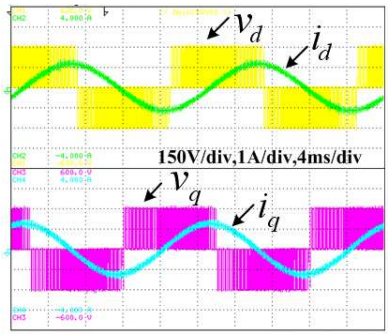

Fig.12: *Two-phase output voltages* (v_d, v_q) *and* $i_d, i_(q)$ *corresponding currents*

Figs.14-15 show harmonic voltage spectrum in peak values for two-phase outputs which harmonic sidebands for both voltages are similar and around at the multiples of the switching frequency (i.e. 5 kHz, 10 kHz, 15 kHz etc.). The inherent characteristic of the harmonic sidebands is typical for a PWM method. This confirms the correctness of the implemented PWM strategy and the main power circuit

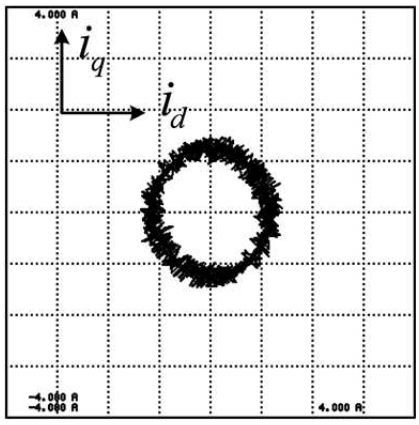

Fig.13: *Current trajectory (1A/div)*

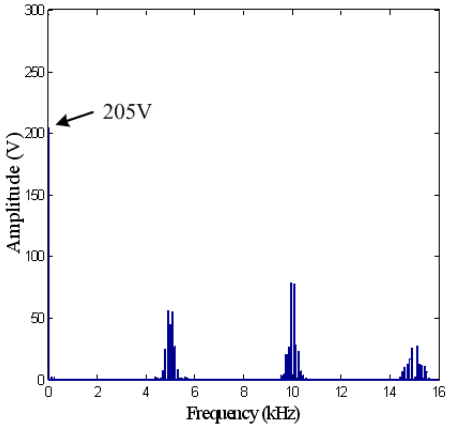

Fig.14: *Measured harmonic voltage spectrum of* v_d

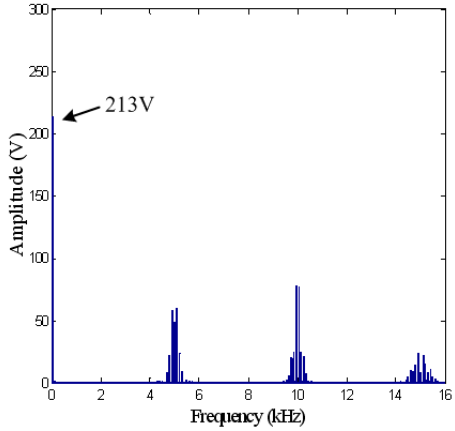

Fig.15: *Measured harmonic voltage spectrum of* v_q

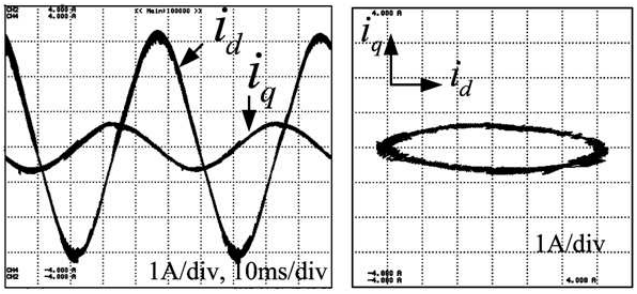

Fig.16: *Two-phase motor currents and space vector trajectory at motor torque of 1.25 Nm.*

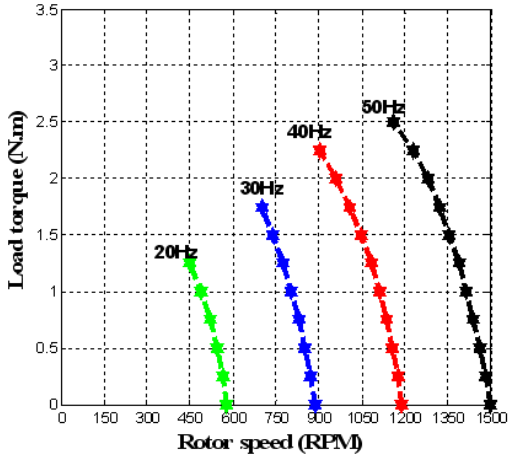

Fig.17: *Torque-speed curves with a variation of inverter frequency.*

operation. The peak fundamental values for both voltages are considerably close. Fig.16 shows the motor current and its trajectory. The amplitude of the main winding current is larger than that of the auxiliary winding current since the impedance of the main winding is lower than that of the auxiliary winding (see Appendix A). As a consequence the trajectory shape is elliptical which the major axis is horizontal. The capability of the proposed system for driving the two-phase asymmetrical induction motor over a wide range of speed is shown in Fig.17. At base inverter frequency (50 Hz), the rated toque is obtained. However when decreasing the inverter frequency, the rated torque could not be reached since the operating slip is greater than the rated slip resulting in overcurrent. It can be seen that at a low speed region, the motor gives a poor capability compared with a high speed region. Therefore it is implied that this motor type needs some control methods such as proposed in [1],[9-10] to improve the better performance particularly at low speed.

5. CONCLUSION

This paper has dealt with the principle and implementation of two-phase SVPWM using a three-leg voltage source inverter providing balanced output voltages. The mathematical equations of space vector equivalent phase leg voltages have been derived. The SVPWM pattern has been implemented by using a DSP board. The correctness of the proposed technique is verified by calculated and experimental results with R-L and motor loads.

References

[1] C.M. Young, C.C. Liu, and C.H. Liu, "New Inverter-Driven Design and Control Method for Two-Phase Induction Motor Drives", *Electric Power Applications, IEE Proceeding*, Vol. 143, No. 6, pp.458-466, 1996.

[2] Y.Cui, F.Blaabjerg and G. Andersen, "An Asymmetrical Space Vector Modulation for Single Phase Induction Motor", *IEEE Proceeding on Industrial Electronics*, Vol.4, pp.1276-1278, 2002.

[3] A.M. Hava, R.J. Kerkman and T.A. Lipo, "Simple Analytical and Graphical Methods for Carrier-Based PWM-VSI Drives", *IEEE Trans. on Power electronics*, Vol.14, pp.2004-2010, 1999.

[4] M.A. Jabbar, A. shwin, M. Khambadkone, and Zhang Yanfeng, "Space-Vector Modulation in a Two-Phase Induction Motor Drive for Constant-Power Operation", *IEEE Trans. on Industrial Electronics* , Vol.51, No. 5, pp.1081-1088, 2004.

[5] D.C. Martins, L.C. Tomaselli, B. Telles, Lazzarin, and Ivo Barbi, "Drive for a Symmetrical Two-phase Induction Machine Using Vector Modulation", *IEEJ Trans. on Industry Applications*, Vol.126, No.7, pp.853-840, 2006.

[6] D. H. jang and D.Y. Yoon, "Space-vector PWM Technique for Two-Phase Inverter-Fed Two-Phase Induction Motors", *IEEE Trans. on Industry Applications*, Vol.39, No. 2 , pp.542-549, 2003

[7] F.C. Lin and S.M. Yang, "Two-Phase Linear Stepping Motor Control With Three-Leg VSI and On-Line Dead-Time Compensation", *Journal of the Chinese Institute of Engineering*, Vol. 28, pp.967-975, 2005.

[8] D. G. Holmes and T. A. Lipo, "Pulse Width Modulation for Power Converters", *Wiley Interscience, IEEE Press*, pp.259-270, 2003.

[9] D.G. Holmes, and A. Kotsopoulos, "Variable Speed Control of Single and Two Phase Induction Motors Using a Three Phase Voltage Source Inverter", *IEEE Conference on Industry Applications*,Vol.1, pp.613-620, 1993.

[10] S. Sinthusonthichat, and V.Kinnares, "A New Modulation Strategy for Unbalanced Two Phase Induction Motor Drives Using a Three-Leg Voltage Source Inverter", *IEEJ Trans. , on Industry Applications*, Vol.125, pp.482-491, 2005.

[11] D.R.Correa, M.B., C.B. Jacobina, A. M. N.

Lima and D. Silva, E.R.C, "A Three-Leg Voltage Source Inverter for Two-Phase AC Motor Drive Systems", *IEEE Trans. on Power Electronics* , vol. 7, No. 14, pp.517-523, 2002.

[12] K. Zhou and D. Wang, "Relationship between Space-Vector Modulation and Three-Phase Carrier-Based PWM: A Comprehensive Analysis", *IEEE Trans. on Industrial Electronics*, vol. 49, No. 1, pp.186-196, 2002.

Appendix A: *Parameters of the asymmetrical two-phase induction motor.*

$1\phi, IM, 370W, 220V, 1375rpm, 2.8A, \alpha = 1.71$		
	Main winding	Auxiliary winding
R_1	9.04Ω	45.25Ω
X_1	13.73Ω	44.79Ω
R_2	7.56Ω	26.76Ω
X_2	6.87Ω	22.40Ω
X_m	234.96Ω	288.20Ω

Chakrapong Charumit received the B.Eng. Degree in electrical engineering from Mahanakorn University of Technology, Bangkok, Thailand, and received the M.Eng. Degree in electrical engineering from King Mongkut's Institue of Technology Ladkrabang, Bangkok, Thailand. He is pursuing the D.Eng degree at King Mongkut's Institue of Technology Ladkrabang. He is currently a lecturer in the Electrical Power Engineering Department, Faculty of Engineering, Mahanakorn University of Technology.

Vijit Kinnares received the B. Eng. and M.Eng. degrees in electrical engineering from King Mongkut's Institue of Technology Ladkrabang, Bangkok, Thailand and the Ph.D. degree from the University of Nottingham, UK. He is currently an Associate Professor in the Electrical Engineering Department, Faculty of Engineering, King Mongkut's Institue of Technology Ladkrabang, Bangkok, Thailand. His research interests are in the fields of electrical machines and electric drives